Journal of Applied Polymer Science

Effect of Air Gap on Gas Permeance/Selectivity Performance of BTDA-TDI/MDI CoPolyimide Hollow Fiber Membranes

Evangelos P. Favvas,[1,2] Sergios K. Papageorgiou,[1] John W. Nolan,[2] Konstantinos L. Stefanopoulos,[1] Athanasios Ch. Mitropoulos[2]

[1]Department of Physical Chemistry, NCSR "Demokritos", Athens, Greece

[2]Department of Petroleum and Natural Gas Technology, Cavala Institute of Technology, St. Lucas, Kavala, Greece

Correspondence to: E. P. Favvas (E-mail: favvas@chem.demokritos.gr)

ABSTRACT: Fabrication, morphology evaluation, and permeance/selectivity properties of three asymmetric BTDA-TDI/MDI copolyimide hollow fiber membranes (HFMs) are reported. The asymmetric HFMs were spun using the dry/wet phase inversion process. The effect of one of the major spinning parameters, the air gap, on the permeance/selectivity properties of the produced HFM was investigated. Scanning electron microscopy was used to evaluate the morphological characteristics and the macroscopic structure of the developed HFM. The permeance values of He, H_2, CH_4, CO_2, O_2, and N_2 gases were measured by the variable pressure method at different feed pressures and temperatures and the permselectivity coefficients were calculated. The higher selectivity values were evaluated for the M1 membrane and were found to be 49.33, 2.99, 5.13, 5.57, and 9.61 for H_2/CH_4, O_2/N_2, CO_2/CH_4, CO_2/N_2, and H_2/CO_2 gas mixtures, respectively. The selectivity experiments of H_2/CH_4, CO_2/CH_4, and O_2/N_2 mixtures were performed at 25°C.
 J. Appl. Polym. Sci. 130: 4490–4499, 2013

KEYWORDS: co-polyimide hollow fiber membranes; effect of air gap; spinning conditions; gas permeance; gas selectivity

Received 11 March 2013; accepted 20 June 2013; Published online 24 July 2013

DOI: 10.1002/app.39677

INTRODUCTION

In plurality of the chemical, pharmaceutical, petrochemical, and oil industries, separation is at the heart of most processes. The most popular natural separation techniques are distillation, extraction, crystallization, sorption, and separations using membranes. In case of membranes, the low operating cost of membrane-based technologies means that they are in the front line of research priorities in materials science and chemical engineering. At this point, it is worth noting that hybrid technologies, such as pressure swing adsorption (PSA) and employing membranes are being evaluated in pilot plants units with the prospect to be utilized in future industrial units.

Baker[1] published an interesting book describing in depth the principles of the membrane technology and applications. During recent years, polymeric membranes have been received a large piece in the membrane research field mainly because of their low manufacturing cost. In addition, synthesis of novel polymers with well-defined structure as "tailored" membrane materials as well as preparation of mixed matrix or composite membranes by various polymeric materials can be easily achieved. In particular, during the last few decades, many research groups around the world have been working on the preparation and performance-testing of polymeric membranes, in flat, spiral wound, and hollow fiber conformations. Polymeric membranes can be used in many application processes such as desalination,[2,3] water purification,[4,5] heavy metal removal,[6,7] hemodialysis,[8,9] natural gas, and olefin/paraffin separation,[10] and so on. Gas separation research using polymeric membranes is a very interesting field, both scientifically and industrially. Current industrial membrane gas separation technologies use glassy and rubbery polymers. The most popular glassy polymers in membrane separation technology are cellulose acetate,[11] polyimides,[12,13] polysulfone,[14,15] polycarbonates,[16] poly(phenylene oxide),[17] polydimethylosiloxane, PDMS,[18] and amide copolymers.[19]

Polyimide is one of the most discussed polymers used in by membrane community. Polyimides are polymers with good thermal properties (T_g around 300°C), they are easily molded into different configurations (flat, hollow, and fiber). In addition, they are cheap and they also have good mechanical properties. It should also be noted that polyimide membranes are one of the most suitable precursors for preparing carbon molecular sieve membranes and many studies have been published in this field.[12,20–24] One of the most promising membrane configurations is that of the hollow fiber because of its extremely high "active" area per volume (module characteristic) which can be spread up to 12,000 m^2/m^3.

To this end, the effect of the spinning conditions on the permeance as well as on the structural characteristics of the produced hollow fiber membranes were reported in a plurality of articles in the literature. In particular, Aptel et al.[25] published, in 1985, the effect of the spinning conditions on ultrafiltration properties of PS hollow fiber membranes. In this study, the researches have found that the increase of the air gap affects negatively the hydraulic permeability coefficient, whereas the increase of the bore liquid flow has positive effect in the hydraulic permeability coefficient. Chung and Hu[26] reported that in case of PES hollow fiber membranes, the increase of the air gap results in a hollow fiber with a less layer of fingerlike voids, a significant lower permeance and a lower T_g. More specifically, Clausi and Koros[27] have prepared defect-free polyimide hollow fiber membranes for gas separations and they concluded that interfacial phase separation in the air gap, as suggested by the dry/wet process, was not likely responsible for the high selectivities exhibited by these fibers. Kapantaidakis et al.[28] studied the effect of spinning conditions on both the structure and the gas permeation properties of high-flux PES/PI blend hollow fibers and they found that the air gap has positive effect on the gas permeance properties. Similarly, the increase of the solvent concentration in bore liquid gives more permeable characteristics on prepared PES/PI membranes. In addition, other researchers have published similar studies in various polymeric hollow fiber membranes. Recently, in 2011, Hasbullah et al.[29] published the gas separation performance of the PANI asymmetric hollow fiber membranes. In this system, when the air gap was increased from 2.5 to 50 cm, the flux for all the test gases showed considerable decrease of about 88–94%. In 2009, Peng et al.[30] studied the rheology of Torlon® solutions and its role in the formation of ultra-thin defect-free Torlon® hollow fiber membranes for gas separation. They concluded the following: (a) spinnerets with narrower spinneret dimension or hollow fibers with smaller thickness will facilitate the formation of macrovoid-free morphology, (b) as the spinneret dimension increases, a higher draw ratio is required to produce defect-free as-spun Torlon® hollow fibers, and (c) a certain air gap may be needed for the fabrication of gas separation membranes with high separation performance to offset the die swell effect. During the same year, Peng et al.[31] have also published an article, focusing on the role of additives on dope rheology and membrane formation of ultra-thin defect-free Torlon® hollow fibers for gas separation. Many interesting conclusions have been exported from this study, such as: (a) as water and ethanol can form hydrogen bonds with Torlon®, the addition of water and ethanol could enhance polymer chain entanglement and form big polymer clusters, (b) the elongational viscosity of Torlon® solutions is the most significant force in determining the molecular orientation in moderate-speed hollow fiber spinning, (c) the rate of stress relaxation and pressure release is another characteristic property of spinning dopes, which is influenced by both the hydrogen bonding and the compressibility of the additives, and (d) hydrogen bonding, polymer cluster size, shear/elongational viscosity, stress relaxation, and pressure release are independent but correlative rheological factors that determine the hollow fiber formation. They function complimentarily with each other during phase inversion. On the other hand, a combination of experimental and theoretical work for understanding the effect of the air gap on the fabrication of hollow fiber membranes was reported by Chung et al.[32] in 1999. Finally, it is worth mentioning that polymeric hollow fiber membranes have also been studied as precursor materials for high-gas-selective carbon hollow fiber molecular sieve membranes. To this end, polyimide hollow fiber membranes have been reported in our previous studies as a promising materials for hydrogen production, O_2/N_2 separation, etc.[12,20,21] Recently, in 2013, He and Hägg have tested the cellulose acetate as a candidate material to propose the derivative carbon hollow fiber membranes for industrial-scale HFCM applications for CO_2 capture.[33]

This study describes a method to prepare BTDA-TDI/MDI copolyimide hollow fiber membranes using the dry/wet spinning approach. The spinning conditions are the critical parameters responsible for the final morphological, mechanical, and physicochemical characteristics of the produced membranes. The most important parameters are (i) the polymer concentration, (ii) the air gap, (iii) the bore liquid composition, (iv) the take-up velocity, (v) the dope flow rate, (vi) the bore liquid flow rate, and (vii) the temperatures of both dope solution and coagulation bath. The study of the effect of all these parameters is a very laborious and time-consuming work. Therefore, in this study, we undertook the task to study the effect of air gap by keeping all the other parameters fixed to monitor the changes on the permeance/selectivity properties. To this end, three polymeric BTDA-TDI/MDI copolyimide hollow fiber membranes were prepared in such a way that the air gap was 0, 6, and 10 cm, respectively (Table I). Both the characterization and the performance evaluation of the membranes were carried out by means of scanning electron microscopy (SEM), single gas permeance of pure gases (*He*, H_2, O_2, N_2, CO_2, *and* CH_4) and gas selectivity (H_2/CH_4, CO_2/CH_4, *and* O_2/N_2) measurements. In addition, the permeance activation energies of the three membranes were calculated in cases of He, O_2, N_2, and CO_2 gases and compared to the literature.

EXPERIMENTAL

Preparation of the Hollow Fiber Membranes

The studied copolyimide hollow fiber membranes were prepared by the dry/wet phase inversion process, a process which is based on the spinodal decomposition principle,[34] in a spinning set up which has been described previously.[35] The polyimide powder (Figure 1), BTDA-TDI/MDI copolyimide, (*Lenzing Plastics*) was dried overnight at 120°C under vacuum, prior dissolution to NMP.

The extruded polymeric solution consisted of P84 polymer and NMP solvent in a dope solution composition (P84/NMP) of 28.5% w/v. The spinning dope was mixed overnight at 50°C in a stainless steel vessel. A homogeneous solution was then obtained through a 30-min treatment of the mixture in an ultrasonic bath. The solution was then filtered through a 25-μm sieve diameter metal filter for removing possible impurities present in the raw polymers. Both vessels and the spinneret were thermostated at 50°C to facilitate the flow of the polymer solution. After filtering, the dopes were degassed inside a second stainless steel vessel for 12 h. The bore liquid constituted a

Table I. Experimental Parameters of Spinning Copolyimide Hollow Fiber Membranes

	Dry spinning		Wet spinning
Membrane	*M*1	*M*2	*M*3
Dope solution composition P84/NMP (%)	28.5	28.5	28.5
Bore fluid composition (%) (NMP : H_2O)	70/30	70/30	70/30
Dope flow rate (mL/min)	2.4	2.4	2.4
Bore liquid flow rate (mL/min)	1.6	1.6	1.6
Air gap (cm)	10	6	0
Room temperature (°C)	17.3	17.3	17.3
Relative humidity (%)	36	36	36
Take-up velocity (m/min)	11	11	11
Dope solution temperature (°C)	50	50	50
Coagulation baths temperature (°C)	25	25	25

degassed solution of NMP and deionized water in different ratios. The polymer solution and bore liquid were simultaneously pumped through a tube-in-orifice spinneret using gear pumps and it has the following characteristics: Needle inner diameter (ID) = 0.5 mm, Needle outer diameter (OD) = 0.7 mm, and Orifice ID = 1.2 mm. The extruded fibers entered the coagulation bath, which was filled with tap water at room temperature. The produced fibers were oriented by means of two guiding wheels and pulled by a third wheel into a collecting reservoir. To remove residual NMP, the produced fibers were washed with tap water overnight and then solvent exchanged in glass containers with ethanol for about 12 h.

According to these conditions, six different hollow fiber membranes were produced; the dope solution composition (28.5% w/w), the dope flow rate (2.4 mL/min), the bore liquid flow rate (1.6 mL/min), the room temperature (17.3°C), the relative humidity of the environment (36%), as well as the temperatures of the dope solution (50°C), coagulation baths (25°C), the bore liquid concentration (NMP/H_2O : 70/30), and

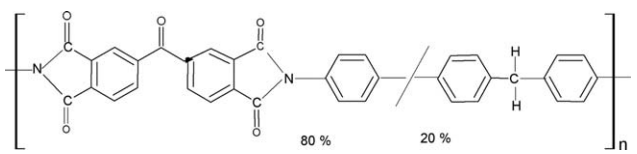

Figure 1. Chemical structure of P84 copolyimide.

the take-up velocity (11 m/min) were kept constant. As a result, the membranes were produced at three different air gaps (10, 6, and 0 cm); the effect of these differences on gas permeance and morphological performance was studied and presented. The experimental parameters of the above hollow fiber membranes produced via spinning technique are listed in Table I.

RESULTS AND DISCUSSION

SEM Analysis

The dimensions and asymmetric structure of the membranes were investigated using a FEI scanning electron microscope. The polymeric fiber samples have been immersed in liquid nitrogen and then they were fractured for their cross-sectional characterization. The produced specimens were mounted on the stub using double-side conductive carbon adhesive tape. Fiber samples were sputter coated with gold using an ion-sputtering device. As summarized in Table II, the dimensions of the hollow fiber membranes, the OD dimension fluctuates from 1040 to 1100 μm, whereas the ID dimension varies between 450 and ~700 μm. In addition, the wall thickness is in the range of ~100–300 μm. These variations are a result of the different spinning conditions and they have been evaluated by the SEM images.

The SEM micrographs of each membrane cross-section (spun under the different air gap outlined in Table I) are shown in Figure 2. At first glance, all the membranes show similar macroscopic characteristics without defects or cracks. They present a cylindrical symmetry and a secondary continuous "dense" layer occurs in the middle of the hollow conformation. The fluctuation of the wall thickness observed for the *M*1 membrane is most likely owing to a long air gap. The existence of the voids (finger-like pores) is the common feature for all studied samples. Additionally, the three separating layers (one on the outer surface, a second at the middle of the wall, and the last one in the inner surface) occur in all membranes, resulting from the specific spinning conditions, the bore liquid composition, the air gap, and the take-up velocity.

A common feature of the three membranes is that their outer diameter is almost equal mainly owing to the geometry of the used spinneret. However, the gravity and the elongation stress, as well as the surface tension are factors that can also affect the dimensions of the fibers. In case of *M*3 membrane, produced via the wet-spinning technique, the wall thickness is approximately 300 μm. This large value of the wall thickness can be attributed to the zero-air gap. Khayet,[36] Qin et al.,[37] and Zhang et al.[38] have also observed that the increase of the air gap results in smaller wall thicknesses in formatted hollow fiber membranes.

A more detailed observation of the *M*2 membrane morphology is shown in Figure 3, where the total cross-section (Figure $3_{(1)}$), the outer skin layer, the inert surface, and the outer surface are presented. This continuous skin layer (Figure. $3_{(2),(4)}$), is responsible for the major permeance characteristics of the membrane. As shown in Figure $3_{(2),(3)}$, a continuous outer layer of about 4 μm lies around the perimeter, which is supported on verticallate sponge-like pores (voids). These macrovoids extend

Table II. OD, ID, and Wall Thickness of the Hollow Fiber Membranes

Hollow-fiber ID	Bore fluid composition (NMP/H_2O)	Air gap (cm)	Take-up velocity (m/min)	OD (μm)	ID (μm)	Wall thickness (μm)
*M*1	70/30	10	11	1100	~700	~200
*M*2	70/30	6	11	1040	640	200
*M*3	70/30	0	11	1050	450	300

from the outer skin layer up to a second continuously "dense" layer nearly to the inner surface of the membrane. Similar smaller finger-like voids meet the inner continuous layer, which is about 1–2 μm thick (Figure $3_{(5)}$). The OD and ID of the *M*2 membrane are 1040 and 640 μm (Figure $3_{(1)}$), whereas the thickness of the outer skin layer, which can be assigned as the separating layer, is about 0.5 μm (Figure $3_{(4)}$). The inner layer's open channels sizes range from 0.07 up to 0.25 μm (±10%) (Figure $3_{(9)}$). The thickness of the continuous channel (macroporous like) layer is usually much greater compared to the size of the external layer because of the presence of a fraction of solvent (NMP) in the bore liquid. For this reason, during the fiber formation, the solvent diffuses more slowly from the bulk to the internal surface and the polymer chains remain in a sponge-type formation. This phenomenon has also been observed by Zhang et al.[39] and Wu et al.[40] in cases of PES- and PVDF/PES-blend hollow fiber membranes. Another interesting morphological feature is the existence of a quite dense interface layer at a distance of about 30 μm from the inner surface of the fiber (Figure $3_{(1)}$). This interface divides the bulk of the fiber into two regions: the inner region with finger-like voids (cavities) ~30 μm length and ~5 μm width, and the outer region with similar cavities ~150 μm length and 7–10 μm width. The occurrence of such an interface layer has also been reported by Yu et al.[41,42] and it reflects the boundary region between the opposite streams of the non solvent (H_2O), diffusing simultaneously from the inner (bore liquid) to the outer (coagulation bath) surface of the fiber.

Gas Permeation–Gas Selectivity Experiments

Single Gas Permeation Experiments. Permeation measurements of various gases (He, H_2, CH_4, CO_2, O_2, and N_2) have been carried out using the variable pressure method in a high-pressure (70 bar) stainless steel permeation rig. This specimen apparatus has been described in detail in the previous studies.[21,43] Before the permeance measurements, the membranes were outgassed for at least 24 h at high vacuum (up to 10^{-6} mbar) at 100°C. Note that the permeance experiments performed in a temperature range of 25–100°C have been repeated after 30 days without a noticeable change in permeance values. Gas was admitted to the high-pressure section of the rig, whereas the low-pressure side remained isolated under vacuum. Permeance experiments were performed by continuously monitoring the pressure increase in the low-pressure side of the rig by means of an accurate differential pressure transducer.

Pure gas permeance values determined using the following formula[44]:

$$\frac{P}{l}=\frac{V\times 273\times 15(p_t-p_0)}{76\times A\times T(1/2)(P_t-P_0)}\times 10^6$$

where the ideal gas law is assumed to be valid. Here, t (s) is the time, p_t (bar) is the pressure at the permeate side at time t, p_0 the permeate pressure at time $t=0$, P (bar) the feed pressure, T (K) the temperature, V (cm^3) the calibrated permeate volume, and A (cm^2) the total membrane area. The gas permeance P/l is expressed in GPU, where 1 GPU = 1 × 10^{-6} cm^3(STP)/(cm^2 s cmHg). The permeability coefficient in Barrer can be estimated by multiplying the gas permeance with the thickness of the dense membrane, l (μm).

The major difference in observed gas separation properties can be attributed to the differences between polymer matrices.[45] For example, the O_2 permeability ranges from 10^4 Barrer for poly(trimethyl silyl propyne) to 10^{-4} Barrers for poly(vinyl alcohol).s However, significant differences in permeance factors were also observed in membranes based on the same polymer but prepared at various conditions. The effect of the preparation conditions in permeability properties of polyelectrolyte

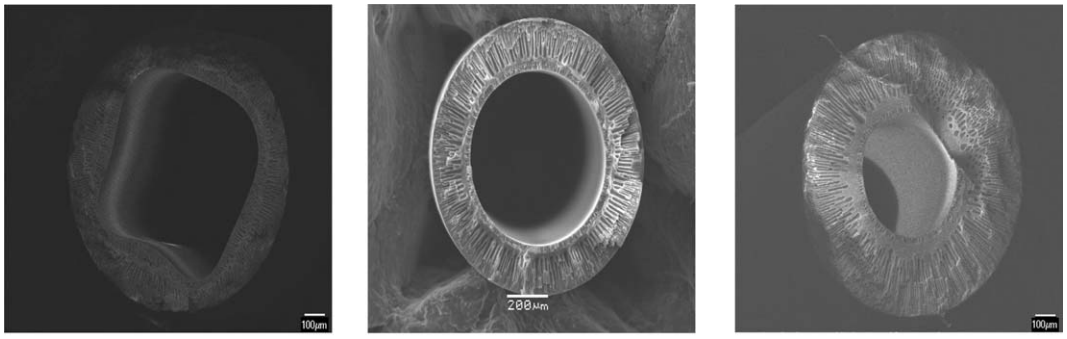

Figure 2. SEM images of the three studied copolyimide hollow fiber membranes (*M*1–*M*3).

Applied Polymer SCIENCE

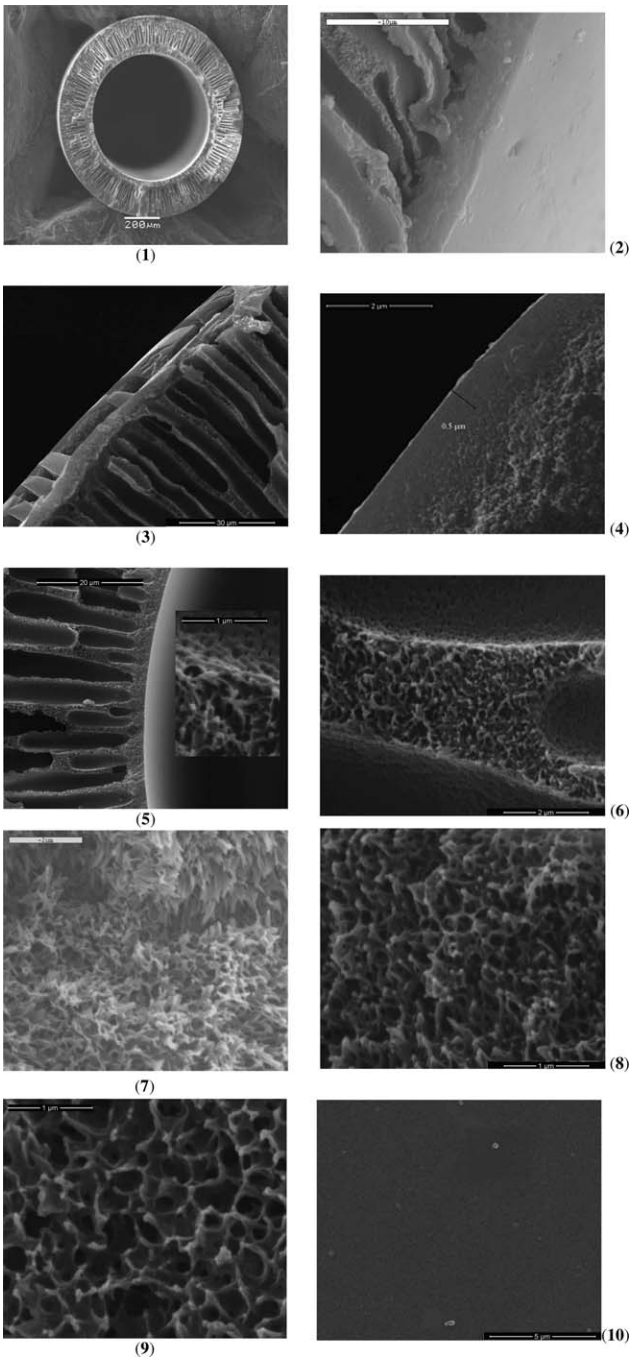

Figure 3. *M*2 hollow fiber membrane: (1–5) Cross-section, (6–9) cross-section in high-resolution analysis, and (10) outer surface.

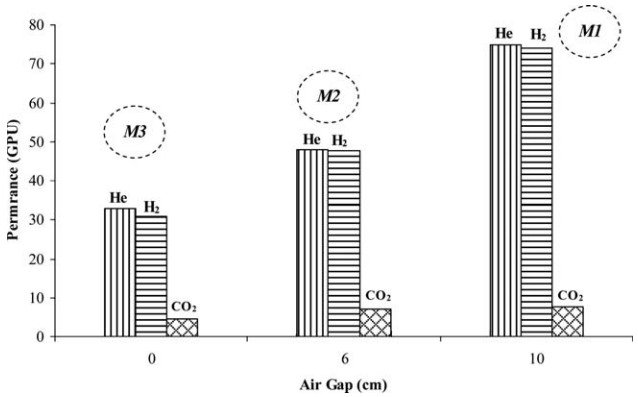

Figure 4. Effect of the air gap on the permeation properties of He, H_2, and CO_2 at 100°C.

complex capsule membranes was reported by Kono et al.[46] Further, the permeance performance characteristics of various PVDF/PVP asymmetric membranes were studied by Munari et al.[47] The effect of both the polymer nature and the membrane preparation conditions on their physicochemical properties has been extensively discussed elsewhere (see Refs. 25,26,28,29,32).

Special care was taken during the experiments to keep the pressure boundary conditions constant. The calculated permeance values are given in GPU and not in Barrer, because the active selective skin layer cannot be determined accurately. As it will be described later, the permeance for each gas is strongly dependent on the air gap, but in all cases, the effect of temperature in gas permeance is positive, especially in the case of smaller molecules and nonadsorbed gases such as helium. The permeance measurements have been carried out for all studied gases at three temperatures, 25, 60, and 100°C, respectively. As shown in Figure 4, in case of helium, hydrogen, and carbon dioxide, that is the gases with the smaller kinetic diameter, the effect of the air gap is positive in gas permeance at 100°C. This was expected owing to the smaller wall thickness and therefore the smaller total resistance in the gas diffusion through the polymeric matrix. On the other hand, the maximum values of permeance for O_2, N_2, and CH_4 were recorded for the *M*2 membrane (air gap, 6 cm). This result can be explained in terms of the different affinities of these molecules with the polyimide matrix. A more detailed explanation is beyond the scope of this study because it demands the calculation of solubility and diffusivity coefficients for each gas. However, it is a motivation for another study in the future.

The elongation of the hollow fiber membranes elongates the microstructure of the polymer chain packing, decreases the polymer density, and results in an increase in the permeance of all tested gases. On the other hand, as Chung and Kafchinski[48] also report that the modification of the air gap has three discernible effects on the hollow fiber membrane formation: (i) influence on the polymer chain orientation (*or even the second phase or nano-fillers, if it exists*), (ii) introduction of extra phase instability, and (iii) accommodation of the phase separation.

As shown in Figure 5, the He permeance is dependent on the temperature. This is typical for activated diffusion mechanism, where the increase in temperature is followed by a similar increase in the permeance. On the other hand, the apparent activation energies for the permeation increase nonproportionally with the increase of the gas molecular sizes.

In general, the permeance values of our membranes can be classified close to an average value when compared with those obtained from the literature. As summarized in Table III, the permeance values (at 25°C) fluctuate from 14.9 to 25.4 GPU for He, 14.4 to 25.3 GPU for H_2, 1.1 to 7.2 GPU for CH_4, 2.2 to

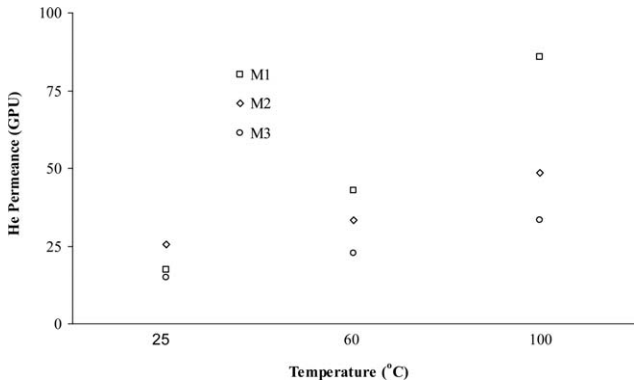

Figure 5. The effect of the temperature on helium gas permeation properties for the three studied P84 hollow fiber membranes.

5.4 GPU for CO_2, 1.3 to 5.6 GPU for O_2, and 0.93 to 6.2 GPU for N_2. Compared with the polyaniline hollow fiber membranes,[29] our samples present similar permeances for N_2, O_2, CO_2, and H_2 in cases of L2.5_1 and L2.5_2 samples but remarkable higher values in cases of L30_1, L30_2, L50_1, L50_2, and L50_3 samples. Our membranes present higher O_2 and N_2 permeances compared with the PBI : PEI blend hollow fiber membranes and smaller permeances for He and H_2.[32] Further, Barsema et al.[44] prepared and characterized highly selective dense and hollow fiber asymmetric membranes based on BTDA-TDI/MDI copolyimide. It is worth mentioning that our membranes, although consisted of the same polymer, present higher permeances for all the studied gases.

All activation energies, for He, O_2, N_2, and CO_2, determined from the slope of each Arrhenius plot, are listed in Table IV. As it can be seen, the ordering of activation energy values in case of He is 9.95 (*M*3), 8.56 (*M*1), and 7.9 (*M*2). Similar results were reported by Dixon-Garrett et al.,[49] Lin and Chung,[50] Bao et al.,[51] and Budd et al.[52] Marked deviations are also observed in the activation energies of permeation (Table IV), except for helium. In addition, negative activation energy values were observed for nitrogen and carbon dioxide. The most pronounced negative activation energy, −3.17 kJ/mol, occurred for CO_2 in the *M*1 membrane. Such negative values have been reported for various polymeric and inorganic membranes in the literature, Dixon-Garrett et al.,[49] Bao et al.,[51] and Budd et al.,[52] and have been explained in terms of the negative influence of temperature on solubility and finally on permeation.[53]

Although the gas permeances increase with temperature, the apparent permeation activation energies increase nonproportionally with the increase in the gas molecular sizes. This happens because in polymeric membranes, the gas diffusion mechanism is completely different compared to inorganic membranes, especially in molecular sieve membranes. Here, the activation energy for permeation is strongly dependent on the chemical affinity and the interactions between the gas molecules and the polymer chains. Gases such as nitrogen and carbon dioxide, whose permeance values are not positively dependent on temperature, present low and even negative permeation activation energies. In particular, as summarized in Table III, the effect of the temperature on the CO_2 permeance can be described as follows: From 25 to 60°C the permeance decreases, whereas from 60 to 100°C increases. Overall, in case of CO_2, the permeance at 100°C is lower than 25°C (from 9.8 GPU drops to 7.7 GPU). The negative values of activation energies for N_2 in case of *M*2 and *M*3 membranes result from the strange behavior of the temperature on the permeance values (Table III). However, for CO_2 the situation is complicated because the effects of diffusion and solubility are opposing each other. Thus, the transport of CO_2 through polyimide can be diffusion controlled when temperature is high and solubility controlled when temperature is low.[54] It is noteworthy that the results summarized in Tables III, V, and VI verify that more permeable polymeric membranes are generally less selective and *vice versa*.[55,56]

The permselectivities are listed in Table V for the following six gas mixtures: H_2/CH_4, O_2/N_2, CO_2/CH_4, CH_4/N_2, CO_2/N_2, and H_2/CO_2. These values were calculated according to the following simple equation:

$$\alpha_{(i/ii)} = \frac{\mathrm{Pe}\left(\mathrm{Gas}_{(i)}\right)}{\mathrm{Pe}\left(\mathrm{Gas}_{(ii)}\right)}$$

It should be noted that these mixtures were chosen for this study because they are relevant to many industrial processes. The development of efficient and new methods of separating gas mixtures into their component parts is needed urgently for two important reasons; first, many gas separations are

Table III. Permeance Values of the Three Membranes at 25, 60, and 100°C[a]

	Permeance (GPU[a])								
	*M*1			*M*2			*M*3		
	25°C	60°C	100°C	25°C	60°C	100°C	25°C	60°C	100°C
He	17.4	43	85.8	25.4	33.4	48.5	14.9	22.8	33.4
H_2	14.4	36.4	74	25.3	33.2	47.7	14.7	21.2	31
CH_4	1.1	1	1.5	7.2	6.7	6.9	2.8	2.8	2.8
CO_2	9.8	4.9	7.7	5.4	6.1	7.2	2.2	3.3	4.4
O_2	1.3	2.06	4.4	5.6	5.6	6.1	2.2	2.4	2.8
N_2	0.93	0.88	1.5	6.2	5.3	5.5	2.2	2.2	2.2

[a] GPU is Barrer without thickness correction.

Table IV. Activation Energies of Permeation (kJ/mol) in Case of He, O_2, N_2, and CO_2 Gases

	Activation energy (kJ/mol)		
Gas	*M1*	*M2*	*M3*
He	8.56	7.9	9.95
O_2	14.97	1.28	3.2
N_2	5.73	−1.55	−0.29
CO_2	−3.17	3.6	8.44

performed on extremely large scales, in numerous industrial processes; improvements will lead to significant global energy savings. Additionally, carbon dioxide capture and storage is an exciting possibility for preventing the release of anthropogenic carbon dioxide into the atmosphere and hinges on gas separations. Detailed analysis of the problem as well as proposed materials and methods can be founded in Yang's book[57] as well as in the article published in 2012 by Herm et al.[58] Furthermore, the need to produce pure hydrogen, especially for use in fuel-cell technologies requires high-cost processes, such as PSA,[59] temperature swing adsorption, and cryogenic processes, as Lee et al. reports.[60] On the other hand, electrical swing adsorption and membrane separation are promising processes for hydrogen production owing to low installation and operational costs. In addition, O_2/N_2 separation is the basic process for oxygen enrichment, preparation of inert gas environments (enhanced nitrogen concentration), etc.

Gas Mixture Testing. The hollow fiber membranes have also been tested in H_2/CH_4, CO_2/CH_4, and O_2/N_2 mixtures separations for evaluating their efficiency in real gas mixture separations. A special apparatus consisting of one stainless steel membrane cell, three mass flow controllers, two pressure transmitters, metal valves, and two back pressure regulators was connected to a high-sensitive HP gas chromatograph. This apparatus was described in detail previously.[61] The membranes were modulated in the special metal cell, forming like a heat-exchanger configuration as shown in Figure 6.

Mixture selectivity experiments were carried out in a high-pressure metal setup. The membranes were attached to a metal tube using a high-vacuum epoxy resin (*Varian, Torr Seal*) and enclosed in a stainless steel permeation cell. The 50/50 (mole concentration) gas mixtures were introduced to the outer side of the membrane, whereas helium was used as the sweep gas on permeate side. Mass flow controllers (Brooks Instruments, 0–50 mL/min) were used to define the flow rates of each gas. In both the retentate and permeate, the pressure was controlled by back-pressure regulators and was recorded using a differential manometer. A Hewlett-Packard 5890 series II gas chromato-

Table V. Ideal Selectivity Coefficients (*permselectivities*) for Six Studied Membranes and for Six Selected Gas Couples at 25, 60, and 100°C

	Permselectivity								
	M1			*M2*			*M3*		
Gases	25°C	60°C	100°C	25°C	60°C	100°C	25°C	60°C	100°C
H_2/CH_4	13.09	36.4	49.33	3.51	4.96	6.91	5.25	7.57	11.07
O_2/N_2	1.40	2.34	2.93	0.90	1.057	1.11	1.00	1.09	1.27
CO_2/CH_4	8.82	4.90	5.13	0.75	0.91	1.04	0.79	1.18	1.57
CH_4/N_2	1.18	1.14	1.00	1.16	1.26	1.25	1.27	1.27	1.27
CO_2/N_2	10.43	5.57	5.13	0.87	1.15	1.31	1.00	1.50	2.00
H_2/CO_2	1.79	7.43	9.61	4.69	5.44	6.63	6.68	6.42	7.05

Table VI. Selectivity Coefficients of Three Gas Pairs for *M1*, *M2*, and *M3* Hollow Fiber Membranes

	M1			*M2*			*M3*		
Gases	25°C	60°C	100°C	25°C	60°C	100°C	25°C	60°C	100°C
Selectivity (50/50 gas mixture)									
H_2/CH_4	9.7	9.2	8.5	1.5	1.4	1.28	2.8	2.5	2.05
CO_2/CH_4	5.5	5.62	5.8	1.9	1.75	1.75	1.2	1.4	1.75
O_2/N_2	2.8	2.65	2.3	1.22	1.13	1.10	1.21	1.42	1.55
Permselectivity									
H_2/CH_4	13.9	36.4	49.33	3.51	4.96	6.91	5.25	7.57	11.07
CO_2/CH_4	8.82	4.9	5.13	0.75	0.91	1.04	0.79	1.18	1.57
O_2/N_2	1.4	2.34	2.93	0.9	1.06	1.11	1	1.09	1.27

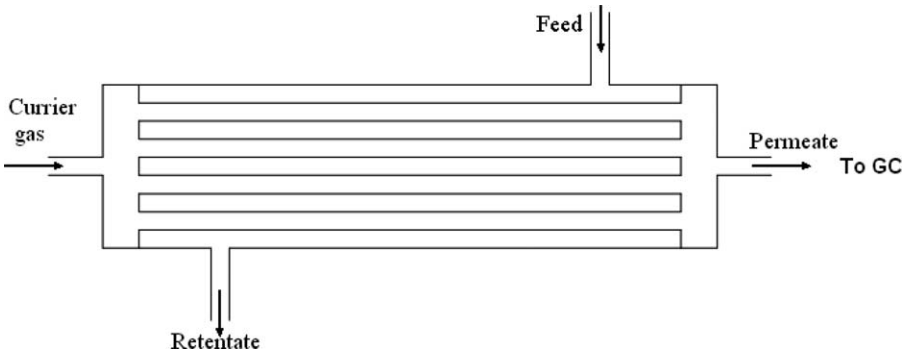

Figure 6. Hollow fiber module for mixture selectivity experiments.

graph equipped with a high-sensitivity TCD detector was used for the analysis of both gas lines.

The selectivity coefficients were calculated according to the follow equation:

$$S=\frac{A_{((\text{gas}-1)-\text{perm})}/A_{((\text{gas}-2)-\text{perm})}}{A_{((\text{gas}-1)-\text{feed})}/A_{((\text{gas}-2)-\text{feed})}}$$

were $A_{((\text{gas}-1)-\text{perm})}$, $A_{((\text{gas}-1)-\text{feed})}$, and $A_{((\text{gas}-2)-\text{perm})}$, $A_{((\text{gas}-2)-\text{feed})}$ are the peak surfaces for the permeate and feed gas streams, respectively.

The selectivities, both measured and calculated, for H_2/CH_4, CO_2/CH_4, and O_2/N_2 at 25, 60, and 100°C, respectively, are listed in Table VI for all the membranes under study. One may notice that the measured selectivity coefficients for the gas pairs H_2/CH_4, CO_2/CH_4, and O_2/N_2 appear either smaller or larger compared to the permselectivities. Mixtures containing hydrogen were found to have lower measured selectivities. Specifically in case of H_2/CH_4 separation, when the membrane is fed with a mixture of hydrogen and methane, the gas mixture selectivity was significantly less than the permselectivity (Table VI). This can be explained in terms of the high methane concentration both in the matrix and on the surface of the membrane, resulting in resistance of the hydrogen diffusion through the membrane. The positive phenomenon occurs in cases of CO_2/CH_4 and O_2/N_2 separations, where the "real" selectivity coefficients are higher than the respective permselectivites. This result has also been reported in case of plasticization action of CO_2 into the polyimide matrix by White et al.[62] and by Wind et al.[63] However, it was observed at pressures above 10 bar. A possible explanation for this behavior could be the fact that the values of both permeance and solubility coefficients of the CO_2 into the polyimide matrix are higher compared with those of CH_4.[64] This means that when CO_2 diffuses into the membrane matrix, the free volume of the polyimide is "saturated" easier by carbon dioxide molecules than by methane molecules and owing to the chemical affinity the diffusion and, thus, the permeation of CO_2 is faster than that of the CH_4. Based on this "swelling" of polyimide chains, the CO_2 concentration is increased into the membrane matrix, the diffusion coefficient is improved and, finally, the effect of CO_2 transport, relevant to CH_4, gives higher CO_2/CH_4 selectivity compared with the correspondent permselectivity. On the same way, the O_2/N_2 selectivities are higher than the corresponded permselectivities because of the better affinity of O_2 with the polyimide chains than the N_2. It is worth mentioning that even these "real" separation factors are "small" and adequate as the studied membranes combine quite satisfactory permeance values in the order of ~70 GPU for H_2 at 100°C.

CONCLUSIONS

This study was devoted to investigate the preparation and the gas performance characterization of asymmetric polymeric hollow fiber membranes prepared with a dry/wet spinning method using commercial P84 copolyimide. In general, the hollow fiber membranes present dimensions of OD between 1040 and 1100 μm, ID between 450 and 700 μm, and wall thickness from 200 to 300 μm. It is worth mentioning that the increase of air gap results in the decrease of the wall thickness. These morphological characteristics were evaluated using SEM. Additionally, the permeation properties for pure gases, and relevant industrial gas mixtures, have been studied extensively. The gas permeances can be classified close to an average value when compared with those obtained from the literature. It was also found that polymeric hollow fiber membranes behave, in many respects, like a typical high free-volume polymer, exhibiting low and even negative permeation activation energies. Further, the gas mixture selectivities have lower values than the calculated ones. However, the opposite is true for the CO_2/CH_4 mixture separation because of the higher solubility and diffusivity coefficients of CO_2 into the polyimide matrix compared with those of CH_4. Conclusively, these hollow fibers can be proved to be excellent candidates for highly selective carbon molecular sieve membranes.

ACKNOWLEDGMENTS

This study is a result in the framework of NSRF. The "NANOSKAI" Project (Archimedes Framework) of the Kavala Institute of Technology is cofinanced by Greece and the European Union in the frame of operational program "Education and lifelong learning investing in knowledge society." Ministry of Education and Religious Affairs, Culture and Sports. NSRF 2007–2013.

REFERENCES

1. Baker, R. W. Membrane Technology and Applications, 2nd ed.; John Wiley & Sons Ltd.: England, **2000**.
2. Curcio, E.; Drioli, E. In Seawater Desalination, Conventional and Renewable Energy Processes; Cipollina, A., Micale, G., Rizzuti, L., Eds.; Springer: Berlin, Heidelberg, **2009**, p 41.
3. Song, L.; Li, B.; Zarkadas, D.; Christian, S.; Sirkar, K. K. *Ind. Eng. Chem. Res.* **2010**, *49*, 11961.
4. Shannon, M. A.; Bohn, P. W.; Elimelech, M.; Georgiadis, J. G.; Mariñas, B. J.; Mayes, A. M. *Nature* **2008**, *452*, 301.
5. Geise, G. M.; Lee, H.; Miller, D. J.; Feeman, B. D.; Mcgrath, J. E.; Paul, D. R. *J. Polym. Sci. Polym. Phys.* **2010**, *48*, 1685.
6. Qdais, H. A.; Moussa, H. *Desalination* **2004**, *164*, 105.
7. Zou, X.; Zhu, G.; Guo, H.; Jing, X.; Xu, D.; Qiu, S. *Micropor. Mesopor. Mater.* **2009**, *124*, 70.
8. Kolf, W. J.; Berk, H. T. *Act. Med. Scandin.* **1994**, *117*, 121.
9. Kolf, W. J. New Ways of Treating Uraemia; J&A Churchill Ltd.: London, **1947**.
10. Askari, M.; Yang, T. X.; Chung, T. S. *J. Membr. Sci.* **2012**, *423*, 392.
11. Gantzel, P.; Merten, U. *Ind. Eng. Chem. Proc. Des. Develop.* **1970**, *9*, 331.
12. Favvas, E. P.; Romanos, G. E.; Papageorgiou, S. K.; Katsaros, F. K.; Mitropoulos, A. Ch.; Kanellopoulos, N. K. *J. Membr. Sci.* **2011**, *375*, 113.
13. Er, O. O.; Sen, S.; Oral, C. A.; Guner, F. S.; Tantekin-Ersolmaz, S. B. *Desalination* **2006**, *200*, 259.
14. Ismail, A. F.; Dunkin, I. R.; Gallivan, S. L.; Shilton, S. *J. Polymer* **1999**, *40*, 6499.
15. Ismail, A. F.; Lai, P. Y. *Sep. Purif. Technol.* **2003**, *33*, 127.
16. Şen, D.; Kalıpçılar, H.; Yilmaz, L. *J. Membr. Sci.* **2007**, *303*, 194.
17. Lin, H.; Freeman, B. D. *J. Membr. Sci.* **2004**, *239*, 105.
18. Panek, D.; Konieczny, K. *Desalination* **2009**, *241*, 197.
19. Liu, L.; Chakma, A.; Feng, X.; Lawless, D. *Can. J. Chem. Eng.* **2009**, *87*, 456.
20. Favvas, E. P.; Kapantaidakis, G. C.; Nolan, J. W.; Mitropoulos, A. Ch.; Kanellopoulos, N. K. *J. Mater. Process. Technol.* **2007**, *186*, 102.
21. Favvas, E. P.; Kouvelos, E. P.; Romanos, G. E.; Pilatos, G. I.; Mitropoulos, A. Ch.; Kanellopoulos, N. K. *J. Porous Mater.* **2008**, *15*, 625.
22. Saufi, S. M.; Ismail, A. F. *Carbon* **2004**, *42*, 241.
23. Salleh, W. N. W.; Ismail, A. F. *Sep. Purif. Technol.* **2012**, *88*, 174.
24. Chen, C. C.; Miller, S. J.; Koros, W. *J. Ind. Eng. Chem. Res.* **2013**, *52*, 1015.
25. Aptel, P.; Abidine, N.; Ivaldi, F.; Lafaille, J. P. *J. Membr. Sci.* **1985**, *22*, 199.
26. Chung, T. S.; Hu, X. D. *J. Appl. Polym. Sci.* **1998**, *66*, 1067.
27. Clausi, D. T.; Koros, W. J. *J. Membr. Sci.* **2000**, *167*, 79.
28. Kapantaidakis, G. C.; Koops, G. H.; Wessling, M. *Desalination* **2002**, *144*, 121.
29. Hasbullah, H.; Kumbharkar, S.; Ismail, A. F.; Li, K. *J. Membr. Sci.* **2011**, *366*, 116.
30. Peng, N.; Chung, T. S.; Lai, J. Y. *J. Membr. Sci.* **2009**, *326*, 608.
31. Peng, N., Chung, T. S.; Li, K. Y. *J. Membr. Sci.* **2009**, *343*, 62.
32. Chung, T. S.; Xu, Z. L.; Lin, W. H. *J. Appl. Polym. Sci.* **1999**, *72*, 379.
33. He, X.; Hägg, M. B. *Chem. Eng. J.* **2013**, *215*, 440.
34. Favvas, E. P.; Mitropoulos, A. Ch. *J. Eng. Sci. Technol. Rev.* **2008**, *1*, 25.
35. Chatzidaki, E. K.; Favvas, E. P.; Papageorgiou, S. K.; Kanellopoulos, N. K.; Theophilou, N. V. *Eur. Polym. J.* **2007**, *43*, 5010.
36. Khayet, M. *Chem. Eng. Sci.* **2003**, *58*, 3091.
37. Qin, J. J.; Li, Y.; Lee, L. S.; Lee, H. *J. Membr. Sci.* **2003**, *218*, 173.
38. Zhang, X.; Wen, Y.; Yang, Y.; Liu, L. *J. Macromol. Sci. B* **2008**, *47*, 1039.
39. Zhang, Y.; Du, Q.; Wu, Y.; Wang, P.; Wu, J. *J. Appl. Polym. Sci.* **2004**, *94*, 259.
40. Wu, L.; Sun, J.; He, C. *J. Appl. Polym. Sci.* **2010**, *116*, 1566.
41. Yu, D. G.; Chou, W. L.; Yang, M. C. *Sep. Purif. Technol.* **2006**, *52*, 380.
42. Yu, D. G.; Chou, W. L.; Yang, M. C. *Sep. Purif. Technol.* **2006**, *51*, 1.
43. Nitodas, S. F.; Favvas, E. P.; Romanos, G. E.; Papadopoulou, M. A.; Mitropoulos, A. Ch.; Kanellopoulos, N. K. *J. Porous Mater.* **2008**, *15*, 551.
44. Barsema, J. N.; Kapantaidakis, G. C.; Van der Vegt, N. F. A.; Koops, G. H.; Wessling, M. *J. Membr. Sci.* **2003**, *216*, 195.
45. Robeson, L. M. *Curr. Opin. Solid State Mater. Sci.* **1999**, *4*, 549.
46. Kono, K.; Ohno, T.; Kumei, T.; Takacishi, T. *J. Appl. Polym. Sci.* **1996**, *59*, 687.
47. Munari, S.; Bottino, A.; Capannelli, G.; Moretti, P. *Desalination* **1985**, *53*, 11.
48. Chung, T. S.; Kafchinski, E. R. *J. Appl. Polym. Sci.* **1997**, *65*, 1555.
49. Dixon-Garrett, S. V.; Nagai, K.; Freeman, B. D. *J. Polym. Sci. Polym. Phys.* **2000**, *38*, 1461.
50. Lin, W. H.; Chung, T. S. *J. Membr. Sci.* **2001**, *186*, 183.
51. Bao, L.; Dorgan, J. R.; Knauss, D.; Hait, S.; Oliveira, N. S.; Maruccho, I. M. *J. Membr. Sci.* **2006**, *285*, 166.
52. Budd, P. M.; McKeown, N. B.; Ghanem, B. S.; Msayib, K. J.; Fritsch, D.; Starannikova, L.; Belov, N.; Sanfirova, O.; Yampolskii, Y.; Shantarovich, V. *J. Membr. Sci.* **2008**, *325*, 851.
53. Pinnau, I.; Z. He. *J. Membr. Sci.* **2004**, *244*, 227.
54. Kim, T. H.; Koros, W. J.; Husk, G. R. *J. Membr. Sci.* **1989**, *46*, 43.

55. Robeson, L. *J. Membr. Sci.* **1991**, *62*, 165.

56. Stern, S. A. *J. Membr. Sci.* **1994**, *94*, 1.

57. Yang, R. T. *Adsorbents: Fundamentals and Applications*; Wiley-Interscience: Hoboken, **2003**.

58. Herm, Z. R.; Krishna, R.; Long, J. R. *Micropor. Mesopor. Mater.* **2012**, *151*, 481.

59. Harrison, D. P. *Ind. Eng. Chem. Res.* **2008**, *47*, 6486.

60. Lee, K. B.; Beaver, M. G.; Caram, H. S.; Sircar, S. *Ind. Eng. Chem. Res.* **2007**, *46*, 5003.

61. Stoitsas, K. A.; Gotzias, A.; Kikkinides, E. S.; Steriotis, Th. A.; Kanellopoulos, N. K.; Stoukides, M.; Zaspalis, V. T. *Micropor. Mesopor. Mater.* **2005**, *78*, 235.

62. White, L. S.; Blinka, T. A.; Kloczewski, H. A.; Wang, I. F. *J. Membr. Sci.* **1995**, *103*, 73.

63. Wind, J. D.; Sirard, S. M.; Paul, D. R.; Green, P. F.; Johnston, K. P.; Koros, W. *J. Macromolecules* **2003**, *36*, 6433.

64. Chern, R. T.; Koros, W. J.; Yui, B.; Hopfenberg, H. B.; Stannett, V. T. *J. Polym. Sci. Polym. Phys. Ed.* **1984**, *22*, 1061.